



Published in final edited form as:

Immunity. 2009 July 17; 31(1): 99–109. doi:10.1016/j.immuni.2009.05.009.

Integrin-Dependent Organization and Bidirectional Vesicular Traffic at Cytotoxic Immune Synapses

Dongfang Liu¹, Yen-an T. Bryceson^{1,2}, Tobias Meckel¹, Gaia Vasiliver-Shamis³, Michael L. Dustin³, and Eric O. Long^{1,*}

¹Laboratory of Immunogenetics, National Institute of Allergy and Infectious Diseases, National Institutes of Health, Rockville, MD 20852, USA

²Center for Infectious Medicine, Department of Medicine, Karolinska Institute, Karolinska University Hospital Huddinge, S-14186 Stockholm, Sweden

³Department of Pathology, New York University School of Medicine, and the Program in Molecular Pathogenesis, Skirball Institute of Biomolecular Medicine, 540 First Avenue, New York, NY 10016, USA.

SUMMARY

Cytotoxic lymphocytes kill target cells by releasing the content of secretory lysosomes at the immune synapse. To obtain information on the dynamics and control of cytotoxic immune synapses we imaged human primary, live natural killer cells on lipid bilayers carrying ligands of activation receptors. Formation of an organized synapse was dependent on the presence of the $\beta 2$ integrin ligand ICAM-1. Ligands of co-activation receptors 2B4 and NKG2D segregated into central and peripheral regions, respectively. Lysosomal protein LAMP-1 that was exocytosed during degranulation accumulated in a large and spatially stable cluster, which overlapped with a site of membrane internalization. Lysosomal compartments reached the plasma membrane at focal points adjacent to centrally accumulated LAMP-1. Imaging of fixed cells revealed that perforin-containing granules were juxtaposed to an intracellular compartment where exocytosed LAMP-1 was retrieved. Thus, cytotoxic immune synapses include a central region of bidirectional vesicular traffic, which is controlled by integrin signaling.

INTRODUCTION

Direct killing of target cells by cytotoxic T lymphocytes (CTL) and natural killer (NK) cells contributes to immune protection from viral infections and cell transformation. CTL and NK cells share a similar mechanism for target cell killing, which occurs through polarized release of the content of cytolytic granules (also called secretory lysosomes) towards the target cell (Orange, 2008; Stinchcombe and Griffiths, 2007). Cytotoxicity proceeds through a number of steps, including integrin-mediated adhesion to target cells, movement of cytolytic granules towards the microtubule organizing center (MTOC), and reorientation of the MTOC towards the target cell. Effector molecules in the cytotoxic pathway include perforin and members of

© 2009 Elsevier Inc. All rights reserved.

*Correspondence Long@nih.gov.

Publisher's Disclaimer: This is a PDF file of an unedited manuscript that has been accepted for publication. As a service to our customers we are providing this early version of the manuscript. The manuscript will undergo copyediting, typesetting, and review of the resulting proof before it is published in its final citable form. Please note that during the production process errors may be discovered which could affect the content, and all legal disclaimers that apply to the journal pertain.

the granzyme family of proteases, which are released upon fusion of cytolytic granules with the plasma membrane, a process also known as degranulation.

Immune synapses were originally described by post-fixation imaging of T cell interactions with antigen-presenting cells (Monks et al., 1998), and by live imaging of T cell interactions with supported planar bilayers presenting ICAM-1 and MHC-peptide complexes (Grakoui et al., 1999). T cell immune synapses include a central region where TCR and CD28 accumulate, and a peripheral region, which includes the $\beta 2$ integrin LFA-1 (CD11a/CD18) (Dustin, 2008). The synapse includes also a focal point for TCR recycling and polarized secretion of cytokines, including interleukin 2 and interferon- γ (Das et al., 2004; Huse et al., 2006), and for delivery of secretory lysosomes towards target cells during T cell cytotoxicity (Stinchcombe and Griffiths, 2007).

Unlike T cells, which express clonally distributed antigen-specific receptors, NK cells can respond in bulk to activation signals. Therefore, it is possible to study the response of primary, unmanipulated human NK cells, isolated directly from peripheral blood. NK cells kill target cells in response to two distinct stimuli: antibody-dependent cellular cytotoxicity (ADCC) through the low affinity Fc receptor Fc γ RIIIA (CD16), and natural cytotoxicity through recognition of ligands on target cells by various NK cell activation receptors (Bryceson et al., 2006a; Lanier, 2005; Moretta et al., 2001). Activation of NK cell cytotoxicity requires the combination of signals for granule polarization and for degranulation. These two signals can be uncoupled in NK cells, as engagement of LFA-1 by its ligand ICAM-1 alone is sufficient to induce granule polarization but not degranulation, whereas degranulation, but not polarization, is induced by CD16 alone (Barber et al., 2004; Bryceson et al., 2005).

Planar lipid bilayers supported on glass coverslips have been used to image immune synapses at high resolution (Dustin et al., 2007). However, the dynamics of vesicular traffic at cytotoxic immune synapses is still poorly defined. To investigate in real time the organization of cytotoxic immune synapses in live degranulating cells we have inserted ligands of NK cell activation receptors into lipid bilayers, and acquired live images by total internal reflection fluorescence (TIRF) microscopy. Ligands for natural cytotoxicity co-activation receptors NKG2D (CD314) and 2B4 (CD244), as well as a ligand for CD16, were used for activation of primary NK cells. The specific contribution of LFA-1 was determined by inclusion of ICAM-1 in the lipid bilayers. Our live images have revealed several properties of cytotoxic immune synapses, all of which are regulated by LFA-1. The ligands of the synergistic co-activation receptors 2B4 and NKG2D segregated into a central and a peripheral region, respectively. The lysosome-associated membrane protein 1 (LAMP-1, also known as CD107a) delivered to the cell surface during degranulation was contained within a central region and retrieved into an intracellular compartment. Finally, perforin-containing cytolytic granules reached the plasma membrane at focal points adjacent to accumulated LAMP-1.

RESULTS

ICAM-1 Imposes a Distinct Ligand Distribution in Cytotoxic NK Cell Immune Synapses

Expression of CD48, a ligand for 2B4, and ULBP1, a ligand for NKG2D, on transfected *Drosophila* Schneider line 2 (S2) cells (Figure S1) was not sufficient to induce degranulation by resting NK cells, as measured by flow cytometry with a CD107a Ab (Figure 1A). However, co-expression of CD48 and ULBP1 on S2 cells induced degranulation (Figure 1A). As shown previously (Bryceson et al., 2005), ICAM-1 did not induce degranulation (Figure 1B). Furthermore, ICAM-1 did not enhance the degranulation induced by CD48, ULBP1, or the combination of CD48 and ULBP1 (Figure 1B).

Primary human NK cells were added to planar lipid bilayers carrying ligands of the three NK cell receptors LFA-1, 2B4, and NKG2D, and the distribution of ligands was imaged by TIRF microscopy. Images of fixed NK cells revealed a characteristic distribution: CD48 accumulated predominantly in the center of the synapse, whereas ULBP1 and ICAM-1 were mainly in a region surrounding the central CD48 (Figure 1C). This organized pattern occurred in all NK cells imaged (> 20 cells). When NK cells were imaged less than 30 minutes after injection onto lipid bilayers, 18 out of 22 imaged cells had an organized synapse (data not shown). Images were also acquired in real time. In this case, all three ligands were again included on the lipid bilayer but only two out of the three were labeled and visualized at a time, as shown with ICAM-1 and ULBP1 (Figure 1D and Movie S1), and ICAM-1 and CD48 (Figure 1E and Movie S2). In agreement with images of fixed cells (Figure 1C), ICAM-1 and ULBP1 were distributed around a central region (Figure 1D and Movie S1), whereas CD48 remained in the center, surrounded by ICAM-1 (Figure 1E and Movie S2). The combination of CD48 and ULBP1, which is sufficient to induce degranulation (Figure 1A), resulted in the distribution of these two ligands into separate clusters, as seen in confocal images of fixed cells (Figure 1F) and in live TIRF images (Figure 1G and Movie S3). NK cells in contact with CD48 and ULBP1 typically assumed elongated shapes. As resting NK cells respond tentatively, it was necessary to search for NK cells that had formed productive synapses.

To test whether a similar synapse organization would occur when NK cells contact a target cell membrane rather than a flat lipid bilayer, fixed conjugates of resting NK cells with transfected *Drosophila* S2 cells were imaged. In this case, the receptors were visualized using Abs to LFA-1, 2B4, and NKG2D. In conjugates with S2-ICAM-1-CD48-ULBP1 cells (Figure S1) 2B4 was distributed more centrally, surrounded by LFA-1 and NKG2D (Figure S2). The distribution of NKG2D was often diffuse rather than peripheral. In conjugates with S2-CD48-ULBP1 cells the distribution of 2B4 and NKG2D was not concentric (Figure S2). Thus, the distribution of receptors on NK cells in contact with target cells was similar to the distribution of their ligands on lipid bilayers. We conclude that co-engagement of LFA-1 is required for the formation of stable, organized synapses. ICAM-1 promoted the accumulation of CD48 in a central region, and partially co-localized with ULBP1 in a peripheral region.

Accumulation of LAMP-1 within a Stable Region at the Center of Cytotoxic Immune Synapses

To test whether degranulation was induced by ligands on lipid bilayers, a directly labeled Fab of a CD107a mAb was included in the lipid bilayer chamber and imaged by TIRF microscopy, as described (Beal et al., 2008). The assay was first validated with NK cells stimulated by Phorbol 12-myristate 13-acetate (PMA) and ionomycin on a lipid bilayer carrying ICAM-1. About 15 minutes after stimulation NK cells acquired CD107a Fab staining (Figure S3A and Movie S4). Clusters of exocytosed LAMP-1 appeared suddenly, and their distribution was dynamic and dispersed over the entire contact area with the lipid bilayer (Figure S3A and Movie S4). As expected for primary, resting NK cells, a sizable fraction of the NK cell population did not degranulate, which provided an internal negative control for CD107a staining (Figure S3A and S3B).

When NK cells were incubated on bilayers carrying ICAM-1, CD48, and ULBP1, a strong CD107a signal accumulated at the center of the synapse (Cells #1, #2, and #3 in Figure 2A). Occasionally, several clusters of LAMP-1 were visible (Cell #4 in Figure 2A). Live imaging revealed that the site of LAMP-1 accumulation was stable over time and space, and acted as an “anchor” for motile NK cells, which were protruding in several directions (Figure 2B and Movie S5). As shown by two-color live imaging, the stable site of LAMP-1 accumulation was contained within peripherally distributed ICAM-1 (Figure 2C). In contrast, on lipid bilayers carrying CD48 and ULBP1 in the absence of ICAM-1, multiple clusters of LAMP-1 remained dispersed over the entire synapse, without central accumulation (Figure 2D and 2E, and Movie

S6). Figure 2F represents time-lapsed imaging of an NK cell in the early phase of degranulation. LAMP-1 staining increased gradually while the NK cell was spreading over the bilayer containing CD48 and ULBP1. We conclude that the accumulation and the confinement of exocytosed LAMP-1 into a stable cluster in cytotoxic synapses are regulated by LFA-1 engagement.

Central Accumulation of LAMP-1 in Synapses Formed over Ligands for LFA-1 and CD16

To compare synapses induced by co-activation receptors for natural cytotoxicity with those induced by CD16, we imaged NK cells over lipid bilayers carrying ICAM-1 and Fc of human IgG1. LAMP-1 released to the surface of degranulating NK cells accumulated in a central region (Cells #1, #2, and #3 in Figure 3A and Movie S7), as it did on lipid bilayers carrying ligands of natural cytotoxicity receptors (Figure 2A). The central accumulation of LAMP-1 was not simply a reflection of membrane accumulation, as shown by double staining with CD107a and the membrane dye DiI16 (Figure S4). Occasionally the distribution of exocytosed LAMP-1 was more dispersed, but formation of a stable cluster of LAMP-1 was still apparent (Cell #4 in Figure 3A, and Movie S8). To test whether the stable LAMP-1 cluster formed through retrieval and accumulation of dispersed exocytosed LAMP-1 or whether it developed at a central point from the outset of degranulation, long-term recordings of individual cells were initiated prior to degranulation. As shown in Figure 3B and Movie S9, at the first appearance of exocytosed LAMP-1, a cluster formed at the site that became the prominent and stable cluster. These results suggest that a central and stable region of LAMP-1 accumulation is in place early during degranulation.

Despite the formation of a stable cluster of exocytosed LAMP-1, ICAM-1 and Fc segregated in separate, disorganized, and unstable clusters (Figure 3C and Movie S10). This was confirmed by imaging fixed cells by confocal microscopy and by two-color live TIRF imaging (Figure S5 and Movie S11). Thus, “ADCC synapses” formed by NK cells over ICAM-1 and IgG1 Fc on lipid bilayers did not have an organized ligand distribution.

As degranulation by resting NK cells is also induced by CD16 signals alone (Bryceson et al., 2005), we imaged cytotoxic synapses formed over lipid bilayers carrying IgG1 Fc. Exocytosed LAMP-1 appeared in multiple dispersed clusters (Figure 3D and Movie S12). The pattern of dispersed LAMP-1 clusters was observed at the very first appearance of exocytosed LAMP-1 at the beginning of degranulation (Movie S13). Occasionally, more extensive clustering of LAMP-1 was observed (Movie S14), particularly at a higher density of Fc (400 – 500 molecules/ μm^2). However, these large LAMP-1 clusters were not spatially and temporally stable (Movies S14), in contrast to the stable clusters formed in the presence of ICAM-1 and Fc. Two-color live imaging revealed that LAMP-1 clusters remained dispersed even when Fc clustered at the center of the synapse (Figure 3E). NK cells injected over lipid bilayers carrying Fc alone not only degranulated, but also promoted rapid and stable clustering of Fc (Figure 3E, Figure S6, and Movie S15). In conclusion, ICAM-1 promoted accumulation of LAMP-1 in a stable cluster after activation of NK cell degranulation by CD16 as well as natural cytotoxicity receptors.

LFA-1 Prevents Diffusion of Exocytosed LAMP-1 and Promotes LAMP-1 Retrieval in a Central Region

Diffusion and retrieval of exocytosed LAMP-1 were evaluated by combining images taken by TIRF and epifluorescence microscopy, within 1 second of each other. If LAMP-1 were free to diffuse at the surface of degranulating cells, it should be visible as a ring under epifluorescence. To test it, we imaged NK cells stimulated by PMA and ionomycin over bilayers carrying ICAM-1. As expected for the receptor-independent degranulation induced by PMA and ionomycin, LAMP-1 was detected in multiple clusters under TIRF, and at the cell periphery

under epifluorescence (Figure 4A). Note that the peripheral distribution of LAMP-1 may include molecules at the cell surface and molecules that have been retrieved by internalization. These results show that receptor-independent degranulation did not lead to accumulation of exocytosed LAMP-1 in a specific region of the cell. In contrast, NK cells that degranulated in response to CD16 in the presence of ICAM-1 retained exocytosed LAMP-1 close to the site of contact, as shown by the lack of staining of the cell periphery under epifluorescence, and by the presence of a central LAMP-1 cluster under TIRF imaging (Figure 4B). Finally, the distribution of LAMP-1 on NK cells that degranulated over lipid bilayers carrying Fc alone was similar to that obtained after stimulation with PMA and ionomycin, and showed that LAMP-1 was not retained within the synapse (Figure 4C). Therefore, engagement of LFA-1 promotes polarized degranulation and prevents the diffusion of exocytosed LAMP-1 around the cell periphery.

An assay developed to measure simultaneously exocytosed LAMP-1 at the cell surface and exocytosed LAMP-1 that has been retrieved into the cell (Bryceson et al., 2005) was used to monitor degranulation and LAMP-1 internalization in the presence or absence of ICAM-1 on S2 insect cells. Activation through CD16 by a rabbit anti-S2 cell serum stimulated exocytosis of LAMP-1 and LAMP-1 internalization (Figure 4D). The diagonal two-color staining for surface and for internalized LAMP-1 indicated that internalization was proportional to LAMP-1 exocytosis. The same balance between LAMP-1 exocytosis and internalization was observed during activation through CD16 in the presence of ICAM-1 (Figure 4D). Therefore, the major control exerted by ICAM-1 on the distribution of exocytosed LAMP-1 and its retrieval into a stable cluster is not due to major changes in the rate of LAMP-1 exocytosis and internalization. Our data supports the conclusion that engagement of LFA-1 by ICAM-1 prevents the diffusion of exocytosed LAMP-1 and promotes its accumulation in a central region of the synapse.

A quantitative analysis was performed by single molecule imaging of CD107a Fab. To relate the fluorescence intensity to the number of Fab molecules, the intensity of single Fab particle signals and of Fab clusters were quantified in the same recordings. CD107a Fab was loaded over the lipid bilayer at different concentrations in the absence of NK cells. Intensities of the diffraction-limited spots had the same distribution, regardless of the concentration of the Fab solution (Figure S7). Such a dilution-independent intensity is only possible for single molecules. The full width at half-maximum (FWHM) was measured as an indicator of the single structure size. Each single Fab followed a Gaussian distribution with a FWHM of 435 ± 17 nm for Alexa Fluor-647, suggesting an imaging resolution of ~ 435 nm (Figure S8). This quantitative analytical approach was applied to determine the number of CD107a Fab molecules per cluster. Most clusters of exocytosed LAMP-1 formed in the absence of ICAM-1 carried a few Fab molecules (11.2 ± 1.7 for CD48+ULBP1, $n=26$, and 10.4 ± 1.1 for Fc, $n=27$), similar to clusters obtained by stimulation with PMA and ionomycin (8.9 ± 2.1 Fab molecules, $n = 28$) (Figure S9). Ten out of 36 clusters induced by CD48 and ULBP1 had 106.8 ± 17.5 Fab molecules, and 2 out 29 induced by Fc had about 55 Fab molecules (Figure S9). However, as shown in Movie S14, these larger LAMP-1 clusters formed in the absence of ICAM-1 were neither spatially nor temporally stable. Addition of ICAM-1 on the bilayer caused a major shift in the number of Fab molecules bound per cluster: namely 214.7 ± 37.5 ($n = 15$) for CD48, ULBP1, and ICAM-1, and 212.7 ± 39.2 ($n = 17$) for Fc with ICAM-1 (Figure S9). Therefore, the presence of ICAM-1 on the lipid bilayer resulted in accumulation of about 20 times more exocytosed LAMP-1 molecules per cluster.

Active Membrane Internalization at the Site of LAMP-1 Accumulation

The stable cluster of LAMP-1 formed in the presence of ICAM-1 may represent accumulation at the cell surface of LAMP-1 molecules that have been exocytosed. However, the recycling

of exocytosed LAMP-1 to intracellular compartments in degranulating cells (Figure 4D) suggested that the central accumulation of LAMP-1 might also correspond to a site of internalization. To visualize membrane internalization in live NK cells, the membrane-impermeable FM1-43 styryl dye was used to label the plasma membrane. FM1-43 inserts into, but does not traverse membranes due to its hydrophilic head (Cousin, 2008). FM1-43 therefore labels the plasma membrane and membranes that have been internalized from the cell surface. FM1-43 can be removed from solvent-accessible membranes by the sulfobutylated derivative of β -cyclodextrin ADVASEP-7 (Kay et al., 1999). To validate this system NK cells and the lipid bilayer were labeled separately with FM1-43 (Figure S10A and S10B). A “destain” with ADVASEP-7 greatly reduced the fluorescence signal (Figure S10A and S10B). To test whether membrane internalization could be observed in live NK cells by this technique, NK cells labeled with FM1-43 were stimulated with PMA and ionomycin, and destained with ADVASEP-7. FM1-43 labeling at the cell periphery was clearly observed before destaining (Figure S10C), whereas internalized membranes visible as distinct vesicles were detected after destaining with ADVASEP-7 (Figure S10C).

The FM1-43 stain-stimulate-destain protocol outlined in Figure 5A was used to visualize membrane internalization in NK cells stimulated on lipid bilayers. NK cells that degranulated in response to PMA and ionomycin showed membrane internalization in multiple compartments, which did not overlap with LAMP-1 clusters (Figure 5B). In live images, both FM1-43-labeled vesicles and LAMP-1 clusters were highly dynamic (data not shown). Stimulation by CD48 and ULBP1 in the presence of ICAM-1 resulted in strong membrane internalization at a site that overlapped with centrally accumulated LAMP-1 (Figure 5C and Movie S16). In contrast, CD48 and ULBP1 in the absence of ICAM-1 induced membrane internalization at multiple, mobile, and dispersed sites, which did not co-localize with clusters of exocytosed LAMP-1 (Figure 5D). Therefore, ICAM-1 promoted the formation of a central region where LAMP-1 accumulated and where membrane was actively internalized. This was also observed after stimulation by Fc and ICAM-1, as a strong FM1-43 signal from internalized membrane overlapped with centrally accumulated LAMP-1 (Figure 5E and Movie S17). The fluorescence intensity of accumulated LAMP-1 and of internalized FM1-43 showed fluctuations over time, indicating dynamic processes. Segregation of internalized FM1-43 and exocytosed LAMP-1 into separate and multiple clusters was observed in NK cells stimulated by Fc alone (Figure 5F and Movie S18), similar to results obtained with NK cells on CD48 and ULBP1 (Figure 5D). Co-localization of internalized FM1-43 and accumulated LAMP-1 was analyzed quantitatively. The Pearson Correlation Coefficient (γ) was 0.29 and 0.28 in the absence of ICAM-1 (Figure 5D and 5F, respectively), and 0.85 and 0.90 in the presence of ICAM-1 (Figure 5C and E, respectively). These data clearly show that the accumulation of LAMP-1 in a stable cluster on NK cells that degranulate in the presence of ICAM-1 corresponds to a site of active membrane internalization.

Lysosomal Compartments Contact the Plasma Membrane at Focal Points Adjacent to Accumulated LAMP-1

The critical role of LFA-1 in promoting granule polarization, organization of NK cell cytotoxic immune synapses, and formation of a region of membrane internalization where LAMP-1 accumulates, suggested that LFA-1 might also control the point at which secretory lysosomes reach the plasma membrane during NK cell degranulation. To test this possibility, lysosomal compartments in primary, live NK cells were labeled with LysoTracker Green DND-26. The pH of lytic granules in NK cells is ~ 4.8 (Liu et al., 2005). The evanescent field, in which the sample is illuminated during TIRF microscopy, is shorter than 200 nm (its calculated value was 87 nm) and decays exponentially with distance from the slide. It is therefore narrower than the diameter of a single lytic granule, which is ~ 400 nm (Burkhardt et al., 1993; Stinchcombe et al., 2001). Therefore, cytolytic granules visible as LysoTracker-positive compartments by

TIRF microscopy would have to be “docked” at, or be very close to the plasma membrane. LysoTracker-loaded NK cells on poly-lysine-coated slides revealed multiple vesicles, some of which moved laterally along the plasma membrane, while others moved into and out of the evanescent field (Figure S11 and Movie S19).

A different picture emerged when lysosomal compartments were imaged in NK cells that degranulated in the presence of ICAM-1. Stimulation by CD48 and ULPB1 induced appearance of lysosomal compartments that remained in close proximity to the stable cluster of LAMP-1 (Figure 6A and 6B, Movie S20 and S21). In the absence of ICAM-1, contacts of lysosomal compartments with the plasma membrane were mobile, dispersed, and not concentrated around LAMP-1 clusters (Figure 6C and 6D, Movie S22 and S23). In NK cells stimulated by Fc and ICAM-1 lysosomal compartments were again adjacent to the stable LAMP-1 clusters (Figure 6E, Movie S24, and Figure S12). In an NK cell that had two LAMP-1 clusters, each one was paired with a stable lysosomal compartment (Figure 6F and Movie S25). In the absence of ICAM-1, membrane-proximal lysosomal compartments and LAMP-1 clusters were mobile and dispersed over a large area of the cytotoxic synapse (Figure 6G and 6H, and Movie S26). The lateral mobility of objects can be rendered in 2-dimension by a “time projection”, which is in effect a z-stack projection where $z = \text{time}$. Time projections for NK cells stimulated by each of the four ligand combinations illustrated how lysosomal compartments at the plasma membrane remained juxtaposed to accumulated LAMP-1 in the presence of ICAM-1 (Figure S13). Kymographs, which depict changes in intensity over time for a given slice through a 2-dimensional image, also illustrated the ICAM-1-dependent stability of adjacent LAMP-1 clusters and lysosomal compartments at the plasma membrane (Figure S14). These results demonstrate that ICAM-1 promotes the formation of focal points in cytotoxic immune synapses where lysosomal compartments reach the plasma membrane and where exocytosed LAMP-1 accumulates.

Perforin-Containing Granules Are Adjacent to Internalized LAMP-1

Three-dimensional imaging of fixed cells was performed to address two main questions: Are the stable LAMP-1 clusters intracellular, and are the adjacent lysosomal compartments cytolytic granules? Resting NK cells incubated in the presence of a CD107a Fab on lipid bilayers carrying ICAM-1 and Fc were fixed and stained with Abs to perforin and tubulin. The stable clusters of LAMP-1 were in large intracellular vesicles (Figure 7A), consistent with data correlating LAMP-1 exocytosis with endocytosis (Figure 4D), and data showing co-localization with internalized membrane (Figure 5C and 5E). Furthermore, perforin-containing granules were juxtaposed to internalized LAMP-1 (Figure 7A), strongly suggesting that lysosomal compartments adjacent to LAMP-1 clusters near the plasma membrane in live cells (Figure 6) were cytolytic granules. Finally, as expected, the MTOC was oriented towards the synapse (Figure 7A). A rotating 3-dimensional view clearly shows that the LAMP-1 compartment and the cytolytic granules are in close proximity of each other and of the lipid bilayer, and that the MTOC is oriented towards the synapse (Movie S27). In the absence of ICAM-1, LAMP-1 clusters were faint and dispersed, and neither perforin-containing granules nor MTOC were polarized towards the synapse (Figure 7B and Movie S28). ICAM-1-dependent polarization of granules and MTOC was also observed in NK cells conjugated with *Drosophila* S2 cells (Figure S15).

To test whether the same LFA-1-dependent distribution of exocytosed LAMP-1 and of cytolytic granules occurred when NK cells were in contact with target cells during natural cytotoxicity, NK cells incubated with S2-ICAM-1-CD48-ULBP1 insect cells in the presence of the CD107a Fab were fixed and imaged by 3-dimensional confocal microscopy. One or two clusters of LAMP-1 were observed at or near the cell surface, and each LAMP-1 cluster was juxtaposed to a perforin-containing granule (Figure S16). Granule polarization was not

observed in NK cells conjugated with S2-CD48-ULBP1 cells. We conclude that cytotoxic immune synapses include an LFA-1-dependent, stable zone where cytolytic granules polarize to fuse with the plasma membrane, and a separate endocytic compartment where LAMP-1 that has been exocytosed during degranulation is retrieved into the cell.

DISCUSSION

Cellular cytotoxicity by T cells and NK cells, a process through which infected or transformed cells are eliminated, is regulated through the formation of stable immunological synapses. In this study, we provided dynamic, high-resolution images of cytotoxic immune synapses formed over lipid bilayers carrying ligands of NK cell activation receptors. Degranulating cells were identified and visualized through appearance of LAMP-1 at the cell surface (Beal et al., 2008). The organization of NK cell cytotoxic immune synapses required the LFA-1 ligand ICAM-1, which promoted segregation of ligands for the synergistic co-activation receptors 2B4 and NKG2D into a central and peripheral region, respectively. A similar organization was observed for the receptors on NK cells during contact with insect cells expressing ligands of human NK cell receptors. ICAM-1 promoted not only spatial organization of receptor–ligand distribution but also the formation of a central zone in the synapse with unique properties. LAMP-1 exocytosed during degranulation did not escape and diffuse over the plasma membrane, but accumulated in a stable, central cluster where membrane internalization occurred. Furthermore, the central region included focal points for the contact of lysosomal compartments with the plasma membrane, which were directly adjacent to accumulated LAMP-1. Three-dimensional reconstructions of cells fixed after degranulation established that perforin-containing granules were in close proximity to a large intracellular compartment containing LAMP-1 recycled from the surface. These results, obtained with primary and unmanipulated NK cells isolated directly from human peripheral blood without exogenous stimuli, reveal that the center of cytotoxic immune synapses is spatially stable and functionally dynamic, as it includes zones of active internalization and exocytosis.

The distribution of receptor–ligand combinations at cytotoxic NK cell immune synapses has unique features. On lipid bilayers, ICAM-1 was distributed preferentially around a central region, similar to its distribution at T cell immune synapses, but the ligands for the synergistic co-activation receptors NKG2D and 2B4 segregated into a peripheral and a central region, respectively. This segregation is somewhat surprising, given that NKG2D and 2B4 require co-engagement to activate resting NK cells ((Bryceson et al., 2006b); and Figure 1A). Although central 2B4 clustering was observed at synapses of transfected NK cells with sensitive target cells (Roda-Navarro et al., 2004), the related receptor CD2 segregated to a peripheral region of NK cell immune synapses (Orange et al., 2003). In other studies using lipid bilayers, mouse CD48 segregated in a zone between the central MHC and ICAM-1 at synapses of mouse T cells over ICAM-1, MHC-peptide, and CD48 (Grakoui et al., 1999). (Note that mouse CD48 binds to both 2B4 and CD2 receptors.) Mouse NK cells on a lipid bilayer carrying ICAM-1 and the NKG2D ligand Rae1 formed a synapse with Rae1 in the center, and ICAM-1 in a peripheral ring (Giurisato et al., 2007). A comparison with human resting NK cells triggered by LFA-1 and NKG2D was not possible because human NK cells crawled actively over bilayers carrying ICAM-1 and ULBP1 (data not shown). The unique, ICAM-1-dependent ligand distribution at human NK cell cytotoxic immune synapses was confirmed with NK cells in contact with insect cells, where 2B4 was preferentially in the center, whereas NKG2D and LFA-1 were peripheral. Our results have revealed an essential role of ICAM-1 in promoting an organized distribution of receptor–ligand pairs at NK cell immune synapses.

The ADCC synapses of NK cells, which involve co-engagement of CD16 and LFA-1, were not organized, as Fc accumulated in multiple dynamic clusters, which overlapped only partially with ICAM-1 clusters. Yet, co-engagement of CD16 and LFA-1 by their respective ligands on

S2 insect cells promoted polarized degranulation and efficient killing (Bryceson et al., 2005). Despite the lack of a discernible receptor–ligand organization, NK cells formed stable ADCC synapses over ICAM-1 and Fc, which were notable for a central region of active LAMP-1 exocytosis and membrane internalization. Therefore, target cell killing by NK cell-mediated ADCC may be quite different from killing by cytotoxic T cells, where LFA-1 and maintenance of an intact p-SMAC may be important for efficient granule-mediated killing by CTL (Anikeeva et al., 2005; Beal et al., 2008; Somersalo et al., 2004).

A striking feature of NK cell cytotoxic immune synapses formed in the presence of ICAM-1 is that LAMP-1 delivered to the cell surface did not escape and diffuse over the plasma membrane. Instead, LAMP-1 accumulated in a large and stable cluster. Imaging of NK cells at the earliest stages of degranulation suggested that ICAM-1 promotes LAMP-1 exocytosis at the center of the synapse, rather than LAMP-1 retrieval from the periphery. In support of this, ICAM-1 did not prevent LAMP-1 diffusion during receptor-independent stimulation of degranulation. During degranulation induced in the absence of ICAM-1, exocytosed LAMP-1 was distributed over the periphery of the entire cell, but remained in microclusters, which would be consistent with a release of cytolytic granule content through partial fusion, without free lateral diffusion of proteins from the granule membrane. By comparison, these LAMP-1 microclusters contained, on average, 20 times less LAMP-1 molecules than the large clusters of LAMP-1 obtained in the presence of ICAM-1.

Live imaging of membranes internalized from the cell surface in the presence of ICAM-1 on the bilayers revealed a central zone of active membrane internalization at the site of LAMP-1 accumulation. Stimulation of NK cells in the absence of ICAM-1 resulted in the distribution of internalized membrane at multiple sites, which did not correspond to micro-clusters of exocytosed LAMP-1. Quantitative degranulation assays with resting NK cells stimulated by S2 insect cells showed that the overall balance of LAMP-1 exocytosis and re-internalization was similar in the presence or the absence of ICAM-1. These results suggest that LFA-1 is not controlling the balance of LAMP-1 exocytosis and re-internalization directly, but prevents LAMP-1 diffusion and promotes accumulation of exocytosed LAMP-1 in a stable and central region of the synapse. Retrieval of LAMP-1 by endocytosis into a central compartment, rather than multiple sites around the cell periphery, could facilitate recycling of lysosomal membranes.

Lytic granules tethered to the plasma membrane have been observed by TIRF microscopy in the NK cell line NK92 (Liu et al., 2005). In the absence of ICAM-1, contacts of lysosomal compartments with the plasma membrane occurred at multiple points within the synapse, which were not stable and not spatially related to micro-clusters of exocytosed LAMP-1. In contrast, in NK cell stimulated in the presence of ICAM-1 on lipid bilayers, LysoTracker-positive compartments formed stable contacts with the plasma membrane at focal points, which were tightly juxtaposed to centrally accumulated LAMP-1. As shown by imaging of fixed cells after stimulation by ligands on lipid bilayers and on insect cells, the large intracellular compartment of recycled LAMP-1 is close to perforin-containing granules.

High-resolution imaging of live and fixed cytotoxic immune synapses has revealed a stable and central zone of bidirectional traffic where cytolytic granules reach the plasma membrane, and where lysosomal membranes, as defined by a high density of LAMP-1 molecules, are retrieved into the cell. This stable region of membrane dynamics is the defining feature of cytotoxic synapses, as it occurred even without an organized distribution of LFA-1 and CD16. Our data so far suggests that traffic proceeds on a divided highway, with little exchange between outgoing and incoming vesicles, although mixing between opposing lanes, as in a two-way street, is likely to occur at some point. The identification of spatially regulated membrane dynamics at the center of NK cell immune synapses induced by two different types

of activation signals suggests that it is a general feature of cytolytic immune synapses, including those of CTL.

EXPERIMENTAL PROCEDURES

Cells

NK cells were isolated from human peripheral blood by negative selection using an NK isolation kit (Miltenyi Biotec, Auburn, CA), and were > 99% CD3⁻CD56⁺. Freshly isolated NK cells were resuspended in Iscove's modified Dulbecco medium (IMDM; Invitrogen, Carlsbad, CA) supplemented with 10% human serum (Valley Biomedical, Winchester, VA) without IL-2, and were used within 2 days.

Antibodies and Reagents

Abs and their source were: 2B4 (clone 2–69, BD Biosciences, San Diego, CA); NKG2D (clone 149810, R&D systems, Minneapolis, MN); CD107a was purified from ascites (clone H4A3, Developmental Studies Hybridoma Bank, University of Iowa, Iowa City, IA); biotinylated CD107a Ab (clone H4A3, BD Bioscience); CD56 mAb (clone NCAM16.2, BD Bioscience); β -tubulin (clone tub2.1, Cy3-conjugated; Sigma-Aldrich); perforin mAb (δ G9, Pierce Chemical Co.); CD11a (clone HI111, BD Bioscience); Alexa Fluor 488-, 568-, and 647-labeled isotype-specific goat anti-mouse Abs (Molecular Probes Inc., Eugene, OR). Phorbol 12-myristate 13-acetate (PMA) and ionomycin calcium salt were from Sigma-Aldrich. The 1, 2-Dioleoyl-sn-Glycero-3-Phosphocholine (DOPC) and 1, 2-Dioleoyl-sn-Glycero-3-[(N-(5-amino-1-carboxypentyl) iminodiacetic acid) succinyl] (Nickel salt) (DOGS-NTA) were from Avanti Polar Lipids, Inc. The acidotropic dye LysoTracker Green DND-26 and membrane dye DiIC16 were from Molecular Probes, Eugene, OR. A 5 mM solution of DiIC16 was made in ethanol and stored at -80°C under argon. Human ICAM-1, CD48, ULBP1, and IgG1 Fc were engineered as soluble molecules fused to a 6-histidine amino acid tag and purified from the supernatants of transfected 293T cells over ProBond Nickel-chelating Resin (Invitrogen). Each protein was further purified by size-exclusion HPLC. Purified His-tagged proteins were labeled with different Alexa Fluor dyes with a protein labeling kit (Molecular Probes, Eugene, OR). CD107a mAb was purified from ascites by Protein A-resin column (Pierce, Rockford, IL). The Fab fragment was prepared with the Immunopure Fab kit (Pierce, Rockford, IL), conjugated with Alexa Fluor 647, and further purified by Sephacryl S-200 size-exclusion HPLC (Figure S7A).

NK Cell Assays

Stimulation with PMA and ionomycin was in 100 nM and 10 μM , respectively. Staining of cell surface and internalized LAMP-1 with CD107a Ab was as described (Bryceson et al., 2005). LysoTracker Green DND-26 was diluted to 50 nM for labeling of lysosomal compartments prior to imaging by TIRFM. 10×10^6 NK cells in 300 μl imaging buffer (HEPES-buffered saline) were injected into FCS2 chambers containing lipid bilayers. Most of the live images were acquired once degranulating NK cells could be identified by appearance of CD107a under TIRF microscopy. As experiments were carried out exclusively with primary, resting NK cells, the time delay between injection into the chamber and detectable degranulation varied considerably among cells and between experimental conditions. The time delays according to stimulation conditions were increasingly longer in the order: PMA and ionomycin, CD16, and NKG2D and 2B4 co-engagement.

Membrane Internalization Assay with FM1-43

Ten million NK cells were washed twice with PBS, incubated at 37°C for 5 min with 8.0 μM FM1-43 in 300 μl imaging buffer (HEPES-buffered saline) containing 0.016 μM Alexa Fluor

647-labeled CD107a Fab, and injected into Biopetechs parallel plate flow chamber-FCS2. For destaining after NK cell activation on lipid bilayers, solvent-accessible FM1-43 was gently stripped for 2 min with 1.0 mM ADVASEP-7 in the imaging buffer with 0.016 μ M Alexa Fluor 647-labeled CD107a Fab.

Supplementary Material

Refer to Web version on PubMed Central for supplementary material.

Acknowledgements

We thank T. Starr, A. Beal, Y. Sykulev, M. March, C. Winter, L. Teyton, S. Radaev, J. Brzostowski, and P. Tolar for advice and help. This work has been supported by the Intramural Research Program of the National Institutes of Health, National Institute of Allergy and Infectious Diseases.

REFERENCES

- Anikeeva N, Somersalo K, Sims TN, Thomas VK, Dustin ML, Sykulev Y. Distinct role of lymphocyte function-associated antigen-1 in mediating effective cytolytic activity by cytotoxic T lymphocytes. *Proc Natl Acad Sci U S A* 2005;102:6437–6442. [PubMed: 15851656]
- Barber DF, Faure M, Long EO. LFA-1 contributes an early signal for NK cell cytotoxicity. *J Immunol* 2004;173:3653–3659. [PubMed: 15356110]
- Beal AM, Anikeeva N, Varma R, Cameron TO, Norris PJ, Dustin ML, Sykulev Y. Protein kinase C θ regulates stability of the peripheral adhesion ring junction and contributes to the sensitivity of target cell lysis by CTL. *J Immunol* 2008;181:4815–4824. [PubMed: 18802085]
- Bryceson YT, March ME, Barber DF, Ljunggren HG, Long EO. Cytolytic granule polarization and degranulation controlled by different receptors in resting NK cells. *J Exp Med* 2005;202:1001–1012. [PubMed: 16203869]
- Bryceson YT, March ME, Ljunggren HG, Long EO. Activation, coactivation, and costimulation of resting human natural killer cells. *Immunol Rev* 2006a;214:73–91. [PubMed: 17100877]
- Bryceson YT, March ME, Ljunggren HG, Long EO. Synergy among receptors on resting NK cells for the activation of natural cytotoxicity and cytokine secretion. *Blood* 2006b;107:159–166. [PubMed: 16150947]
- Burkhardt JK, McIlvain JM Jr, Sheetz MP, Argon Y. Lytic granules from cytotoxic T cells exhibit kinesin-dependent motility on microtubules in vitro. *J Cell Sci* 1993;104(Pt 1):151–162. [PubMed: 8449993]
- Cousin MA. Use of FM1-43 and other derivatives to investigate neuronal function. *Curr Protoc Neurosci* Chapter 2008;2Unit 2 6
- Das V, Nal B, Dujeancourt A, Thoulouze MI, Galli T, Roux P, Dautry-Varsat A, Alcover A. Activation-induced polarized recycling targets T cell antigen receptors to the immunological synapse; involvement of SNARE complexes. *Immunity* 2004;20:577–588. [PubMed: 15142526]
- Dustin ML. T-cell activation through immunological synapses kinapses. *Immunol Rev* 2008;221:77–89. [PubMed: 18275476]
- Dustin ML, Starr T, Varma R, Thomas VK. Supported planar bilayers for study of the immunological synapse. *Curr Protoc Immunol* Chapter 2007;18Unit 18 13
- Giurisato E, Cella M, Takai T, Kurosaki T, Feng Y, Longmore GD, Colonna M, Shaw AS. Phosphatidylinositol 3-kinase activation is required to form the NKG2D immunological synapse. *Mol Cell Biol* 2007;27:8583–8599. [PubMed: 17923698]
- Grakoui A, Bromley SK, Sumen C, Davis MM, Shaw AS, Allen PM, Dustin ML. The immunological synapse: a molecular machine controlling T cell activation. *Science* 1999;285:221–227. [PubMed: 10398592]
- Huse M, Lillemeier BF, Kuhns MS, Chen DS, Davis MM. T cells use two directionally distinct pathways for cytokine secretion. *Nat Immunol* 2006;7:247–255. [PubMed: 16444260]

- Kay AR, Alfonso A, Alford S, Cline HT, Holgado AM, Sakmann B, Snitsarev VA, Stricker TP, Takahashi M, Wu LG. Imaging synaptic activity in intact brain and slices with FM1-43 in *C. elegans*, lamprey, and rat. *Neuron* 1999;24:809–817. [PubMed: 10624945]
- Lanier LL. NK cell recognition. *Annu Rev Immunol* 2005;23:225–274. [PubMed: 15771571]
- Liu D, Xu L, Yang F, Li D, Gong F, Xu T. Rapid biogenesis and sensitization of secretory lysosomes in NK cells mediated by target-cell recognition. *Proc Natl Acad Sci U S A* 2005;102:123–127. [PubMed: 15618404]
- Monks CR, Freiberg BA, Kupfer H, Sciaky N, Kupfer A. Three-dimensional segregation of supramolecular activation clusters in T cells. *Nature* 1998;395:82–86. [PubMed: 9738502]
- Moretta A, Bottino C, Vitale M, Pende D, Cantoni C, Mingari MC, Biassoni R, Moretta L. Activating receptors and coreceptors involved in human natural killer cell-mediated cytotoxicity. *Annu Rev Immunol* 2001;19:197–223. [PubMed: 11244035]
- Orange JS. Formation and function of the lytic NK-cell immunological synapse. *Nat Rev Immunol*. 2008
- Orange JS, Harris KE, Andzelm MM, Valter MM, Geha RS, Strominger JL. The mature activating natural killer cell immunologic synapse is formed in distinct stages. *Proc Natl Acad Sci U S A* 2003;100:14151–14156. [PubMed: 14612578]
- Roda-Navarro P, Mittelbrunn M, Ortega M, Howie D, Terhorst C, Sanchez-Madrid F, Fernandez-Ruiz E. Dynamic redistribution of the activating 2B4/SAP complex at the cytotoxic NK cell immune synapse. *J Immunol* 2004;173:3640–3646. [PubMed: 15356108]
- Somersalo K, Anikeeva N, Sims TN, Thomas VK, Strong RK, Spies T, Lebedeva T, Sykulev Y, Dustin ML. Cytotoxic T lymphocytes form an antigen-independent ring junction. *J Clin Invest* 2004;113:49–57. [PubMed: 14702108]
- Stinchcombe JC, Bossi G, Booth S, Griffiths GM. The immunological synapse of CTL contains a secretory domain and membrane bridges. *Immunity* 2001;15:751–761. [PubMed: 11728337]
- Stinchcombe JC, Griffiths GM. Secretory mechanisms in cell-mediated cytotoxicity. *Annu Rev Cell Dev Biol* 2007;23:495–517. [PubMed: 17506701]

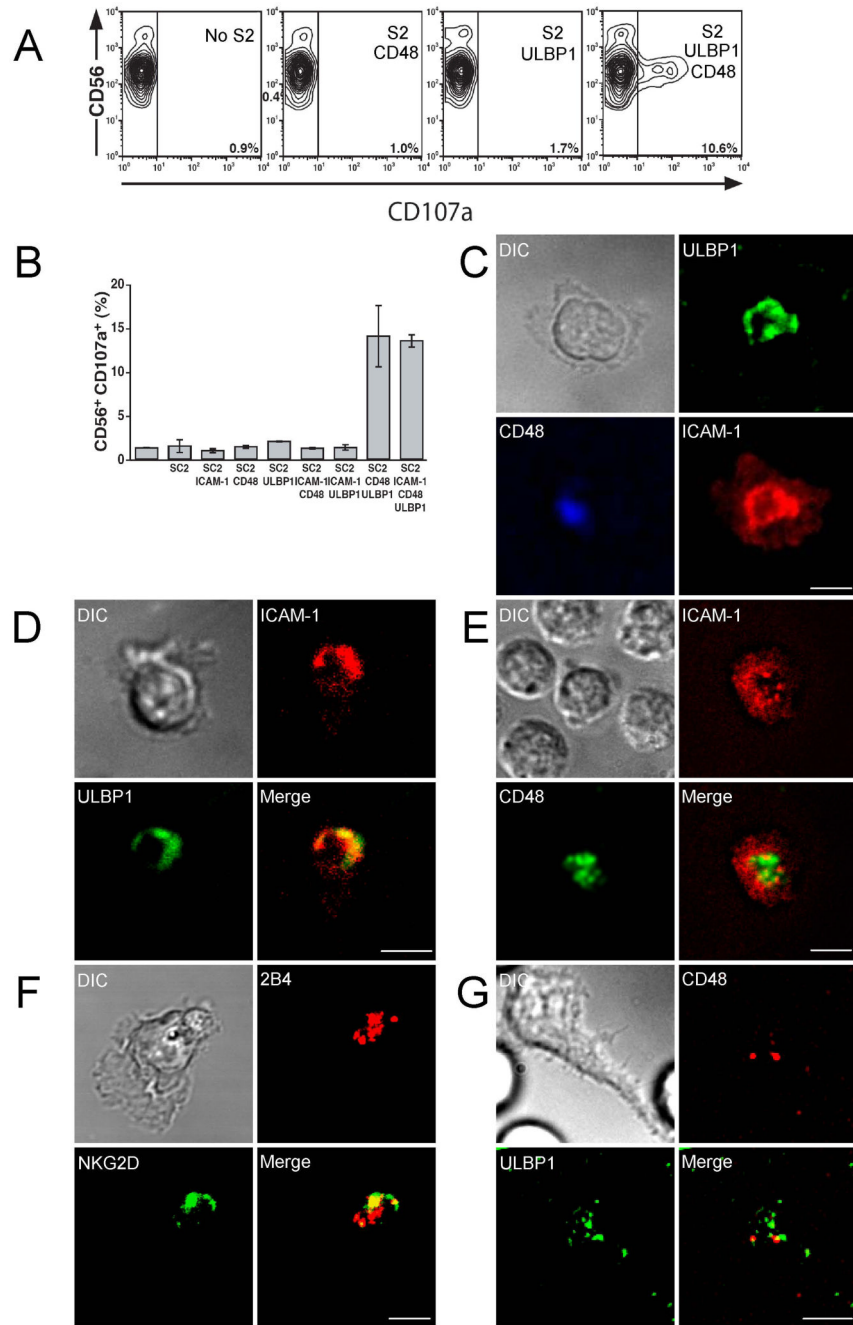


Figure 1. ICAM-1 Controls the Organization of Natural Cytotoxicity Immune Synapses
 Scale bars are 5.0 μ m. The images are representative of at least 20 cells in three independent experiments. (A) CD107a staining of resting NK cells after mixing with S2 insect cells transfected with the indicated ligands. A control without S2 cells is also shown. (B) Percentage of CD107a⁺ NK cells after mixing with the indicated transfected S2 cells. Bars indicate SD of triplicate samples. (C) TIRF image of an NK cell fixed ~60 min after addition to a bilayer carrying ICAM-1-Alexa Fluor 568, ULBP1-Alexa Fluor 488, and CD48-Alexa Fluor 647. (D) TIRF image of a live NK cell at ~60 min after addition to a bilayer carrying ICAM-1-Alexa Fluor 568, ULBP1-Alexa Fluor 488, and unlabeled CD48. (E) TIRF image of live NKs cell at ~130 min after addition to a bilayer carrying ICAM-1-Alexa Fluor 568, CD48-Alexa Fluor

488, and unlabeled ULBP1. (F) Confocal image of an NK cell fixed ~60 min after addition to a bilayer carrying unlabeled CD48 and ULBP1. Fixed and permeabilized cells were incubated with Abs to 2B4 and NKG2D, followed by Alexa Fluor 568 and Alexa Fluor 488 conjugated secondary Abs, respectively. (G) TIRF image of live NK cells at ~90 min after addition to a bilayer carrying CD48-Alexa Fluor 568 and ULBP1-Alexa Fluor 488.

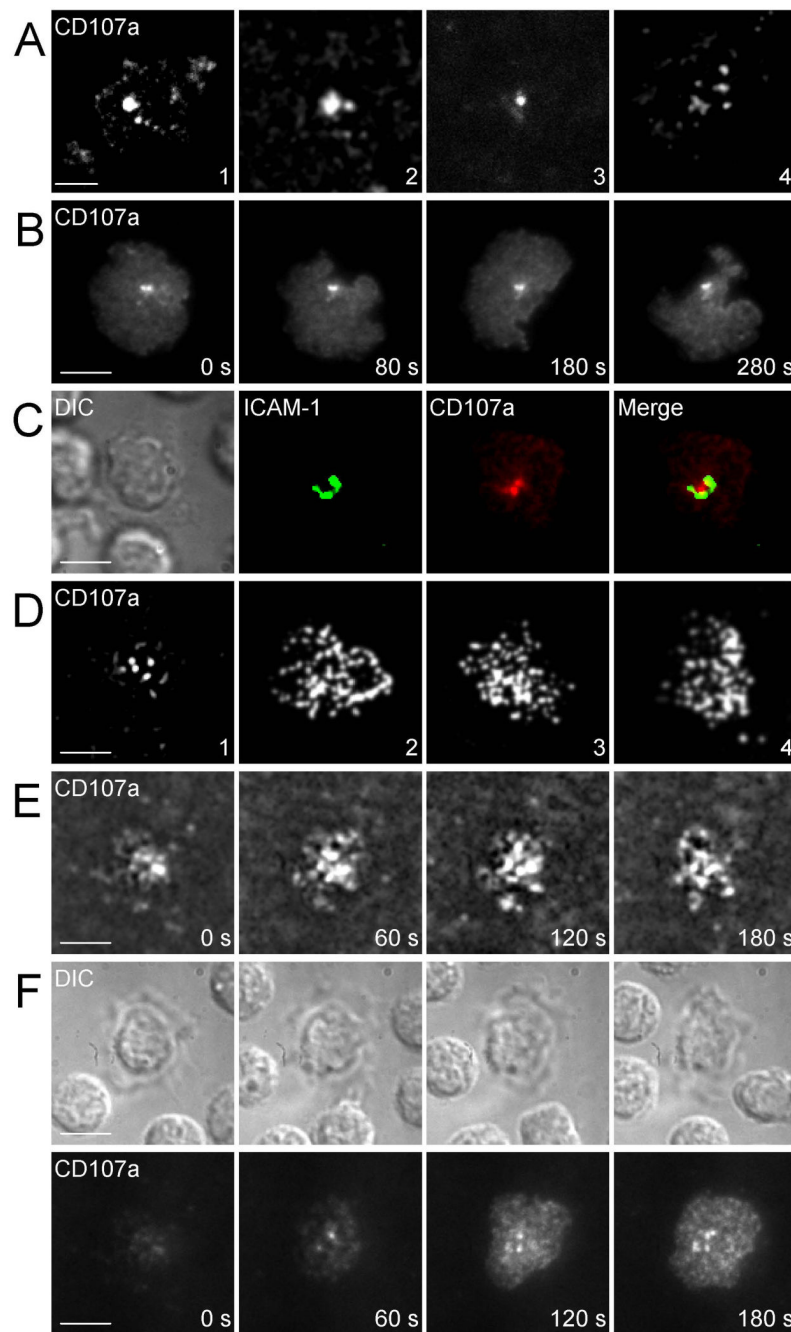


Figure 2. LAMP-1 Accumulates in a Central Cluster within Cytotoxic Immune Synapses
 Degranulation was monitored by TIRFM with a soluble CD107a F(ab) conjugated with Alexa Fluor 647. Scale bars are 5.0 μm . The images are representative of at least 30 cells in five independent experiments. (A to C) Live NK cells imaged on bilayers carrying ICAM-1, CD48, and ULBP1. (A) Individual cells imaged at ~ 100 min (#1), ~ 120 min (#2), ~ 180 min (#3), and ~ 60 min (#4), after addition to the bilayer. (B) Time-lapsed images taken at ~ 120 min after addition of NK cells to the bilayer. (C) NK cells imaged at ~ 120 min after addition to a bilayer carrying unlabeled CD48 and ULBP1 and Alexa Fluor 488 conjugated ICAM-1. (D to F) Live NK cells imaged on bilayers carrying unlabeled CD48 and ULBP1. (D) Individual cells imaged at ~ 90 min (#1), ~ 120 min (#2), ~ 120 min (#3), and ~ 180 min (#4) after addition to the bilayer.

(E) Time-lapsed images taken at ~120 min after addition of NK cells to the bilayer. (F) NK cells imaged ~200 min after addition to the lipid bilayer. Time-lapsed DIC (top panel) and TIRF (bottom panel) images.

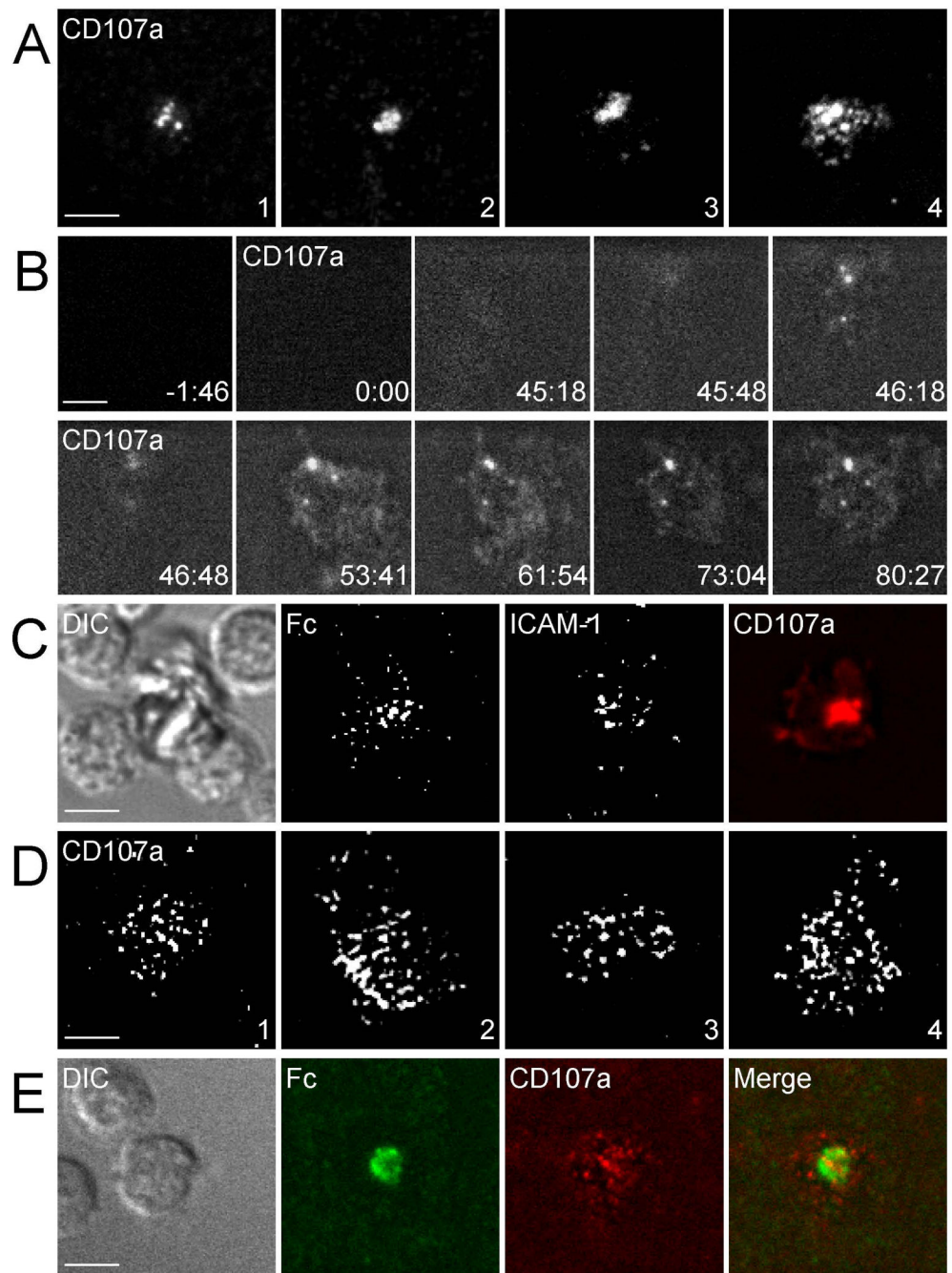


Figure 3. Central Accumulation of LAMP-1 in Synapses Formed over Ligands for LFA-1 and CD16
 Degranulation was monitored by TIRFM with a soluble CD107a F(ab) conjugated with Alexa Fluor 647. Scale bars are 5.0 μ m. The images are representative of at least 50 cells in five independent experiments. (A and B) Live NK cells imaged on bilayers carrying unlabeled ICAM-1 and IgG1 Fc. (A) Individual cells imaged at ~50 min (#1), ~80 min (#2), ~120 min (#3), and ~26 min (#4), after addition to the bilayer. (B) Time series taken from Movie S8. The first frame was taken prior to the addition of CD107a Fab and of NK cells. The second frame was taken at the time of CD107a Fab and NK cell injection into the chamber. (C) NK cells imaged at ~120 min after addition to a bilayer carrying Alexa Fluoro 488 conjugated ICAM-1 and Alexa Fluoro 568 conjugated Fc. (D and E) Live NK cells imaged on bilayers carrying IgG1

Fc alone. (D) Individual cells imaged at ~30 min (#1), ~40 min (#2), ~60 min (#3), and ~100 min (#4) after addition to the bilayer. (E) NK cells imaged at ~30 min after addition to a bilayer carrying Alexa Fluor 488-conjugated Fc.

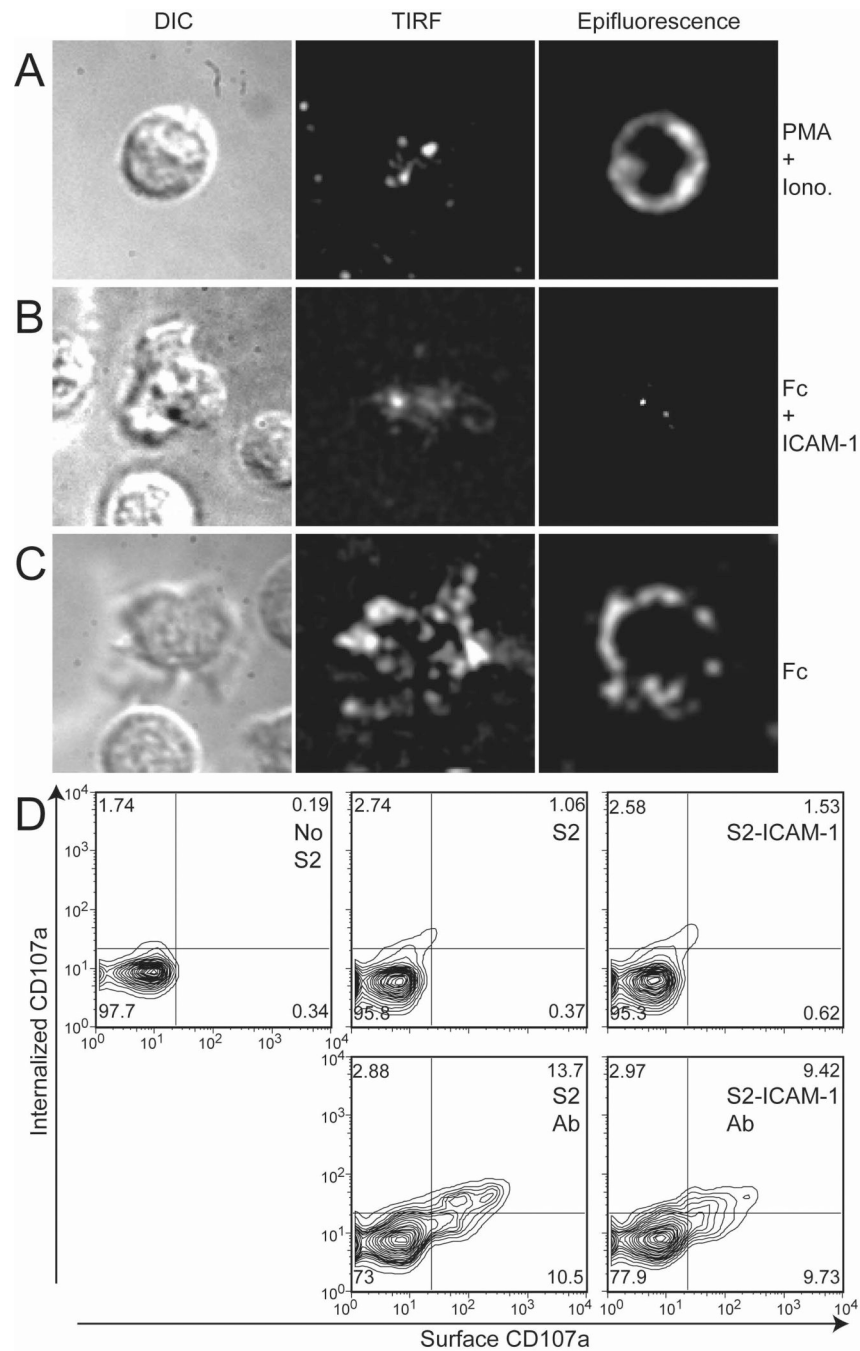


Figure 4. Diffusion of LAMP-1 on Degranulating Cells Is Constrained in the Presence of ICAM-1 (A to C) Live NK cells over lipid bilayers were imaged by DIC, TIRF, and epifluorescence, after incubation with a soluble CD107a F(ab) conjugated with Alexa Fluor 647. The DIC, TIRF, and epifluorescence images were acquired within one second of each other. Scale bars are 5.0 μm . The images are representative of 10 cells in three independent experiments. (A) NK cell on a bilayer carrying unlabeled ICAM-1 imaged 20 min after addition of PMA and ionomycin. (B) NK cells imaged \sim 140 min after addition to a bilayer carrying unlabeled ICAM-1 and Fc. (C) NK cells imaged \sim 37 min after addition to a bilayer carrying unlabeled Fc alone. (D) Staining of extracellular and internalized LAMP-1 with CD107a Ab 2 hours after mixing NK cells with S2 cells, S2 cells transfected with ICAM-1, and S2 cells coated with

rabbit antiserum (Ab), as indicated. NK cells were gated by staining with FITC-conjugated CD56 mAb. Selective staining of internalized LAMP-1 by PE and of cell surface LAMP-1 by allophycocyanin using biotinylated CD107a Ab is described in Experimental Procedures.

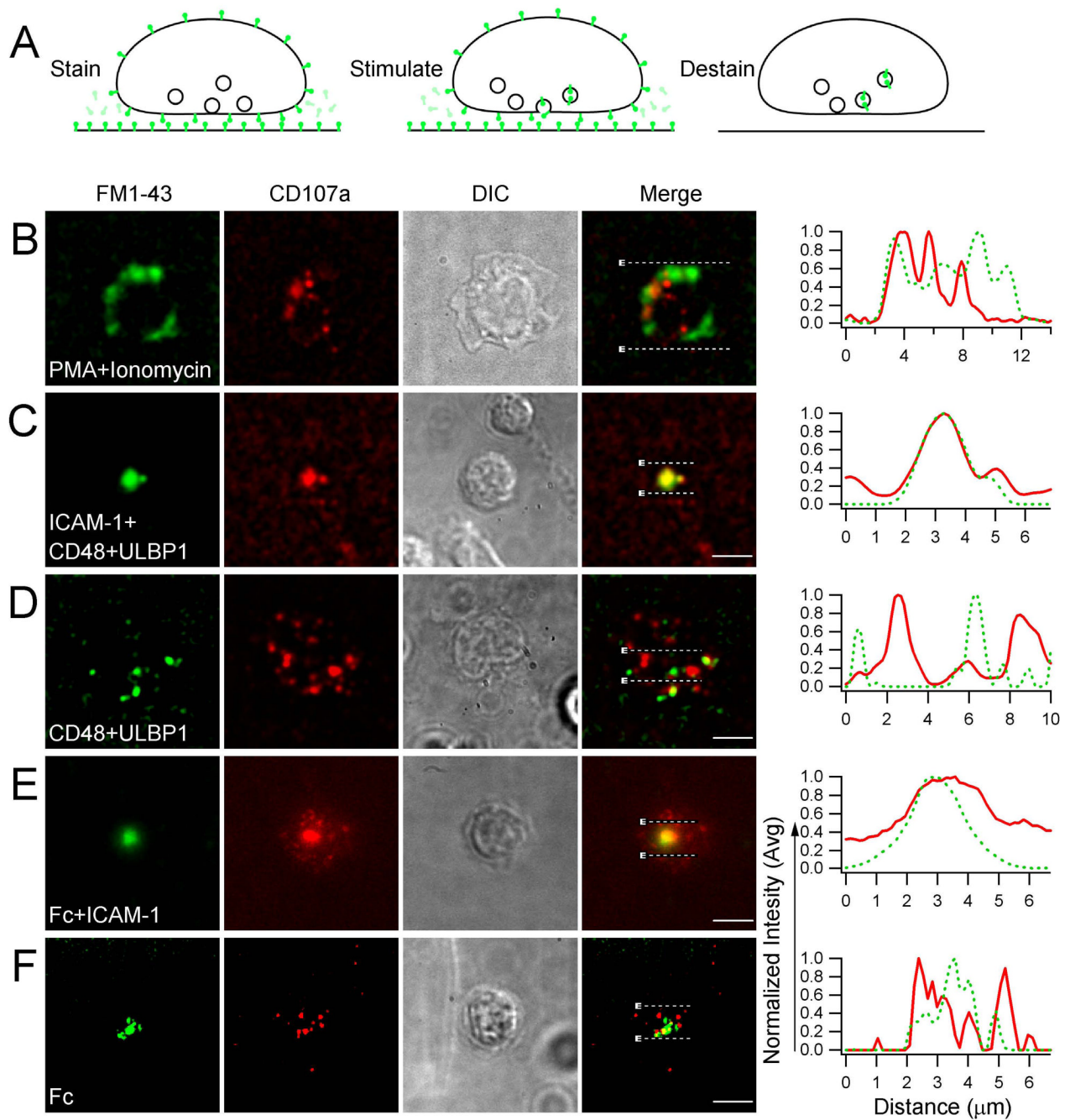


Figure 5. Internalized Membranes Co-Localize with Centrally Accumulated LAMP-1

(A) Internalized membranes in FM1-43-labeled and stimulated NK cells were detected by TIRFM after destaining with ADVASEP-7. FM1-43 has almost no fluorescent properties in aqueous solution. NK cells were incubated with $8.0 \mu\text{M}$ FM1-43 at 37°C for 5 min and injected into Biopetechs chamber for 60 min. For destaining, FM1-43 was stripped for 2 min with 1.0 mM ADVASEP-7. (B to F) Degranulation was monitored by TIRFM with a soluble CD107a F(ab) conjugated with Alexa Fluor 647. The DIC, FM1-43, and LAMP-1 images were acquired within one second of each other. The normalized intensity of CD107a (Red lines) and FM1-43 (Green lines) signals within the parallel horizons indicated in the composites were graphed in the right panels. Scale bars are $5.0 \mu\text{m}$. The images are representative of at least 20 cells in

three independent experiments. (B) PMA and ionomycin-stimulated NK cells imaged ~20 min after addition to a bilayer carrying unlabeled ICAM-1. (C) NK cells imaged ~160 min after addition to a bilayer carrying unlabeled CD48, ULBP1, and ICAM-1. (D) NK cells imaged ~200 min after addition to a bilayer carrying unlabeled CD48 and ULBP1. (E) NK cells imaged ~120 min after addition to a bilayer carrying unlabeled Fc and ICAM-1. (F) NK cells imaged ~60 min after addition to a bilayer carrying unlabeled Fc.

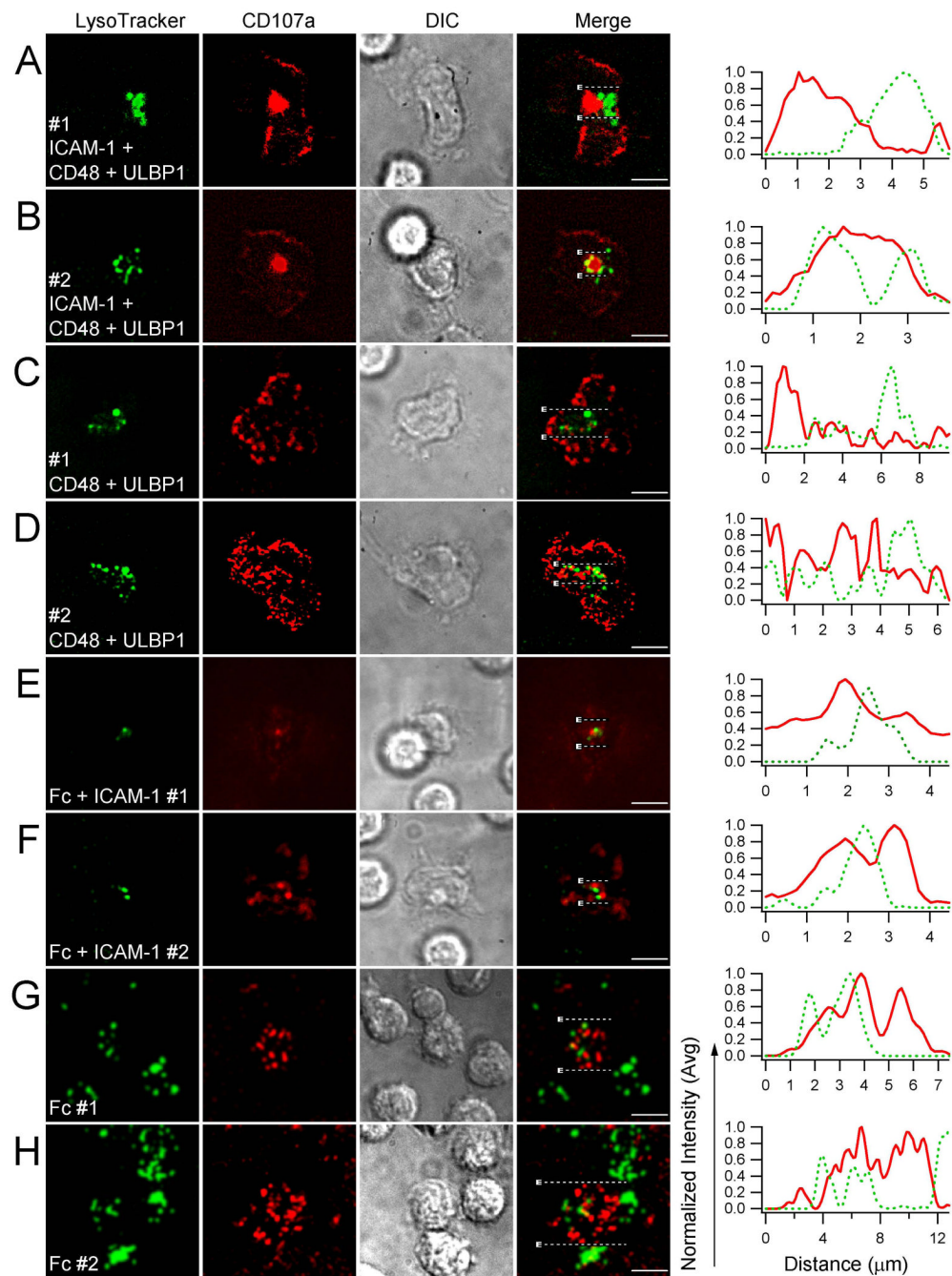


Figure 6. Lysosomal Compartments Reach the Plasma Membrane at Focal Points Adjacent to Accumulated LAMP-1

Scale bars are 5.0 μm . The images are representative of at least 50 cells in three independent experiments. Lysosomal compartments labeled with LysoTracker Green and exocytosed LAMP-1 labeled with a soluble CD107a Fab conjugated with Alexa Fluor 647 were imaged by TIRFM. DIC and TIRF images were acquired within one second of each other. The normalized intensity of CD107a (Red lines) and LysoTracker (Green lines) over the parallel horizon indicated in the merged images are shown in the panels on the right. (A and B) NK cells imaged on bilayers carrying unlabeled CD48, ULBP1, and ICAM-1 ~ 90 min (#1) and ~ 170 min (#2) after injection over the bilayer. (C and D) NK cells imaged on bilayers carrying

unlabeled CD48 and ULBP1 ~88 min (#1) and ~260 min (#2) after injection over the bilayer. (E and F) NK cells imaged on bilayers carrying unlabeled Fc and ICAM-1 ~130 min (#1) and ~50 min (#2) after injection over the bilayer. (G and H) NK cells imaged on bilayers carrying unlabeled Fc ~60 min (#1) and ~130 min (#2) after injection over the bilayer.

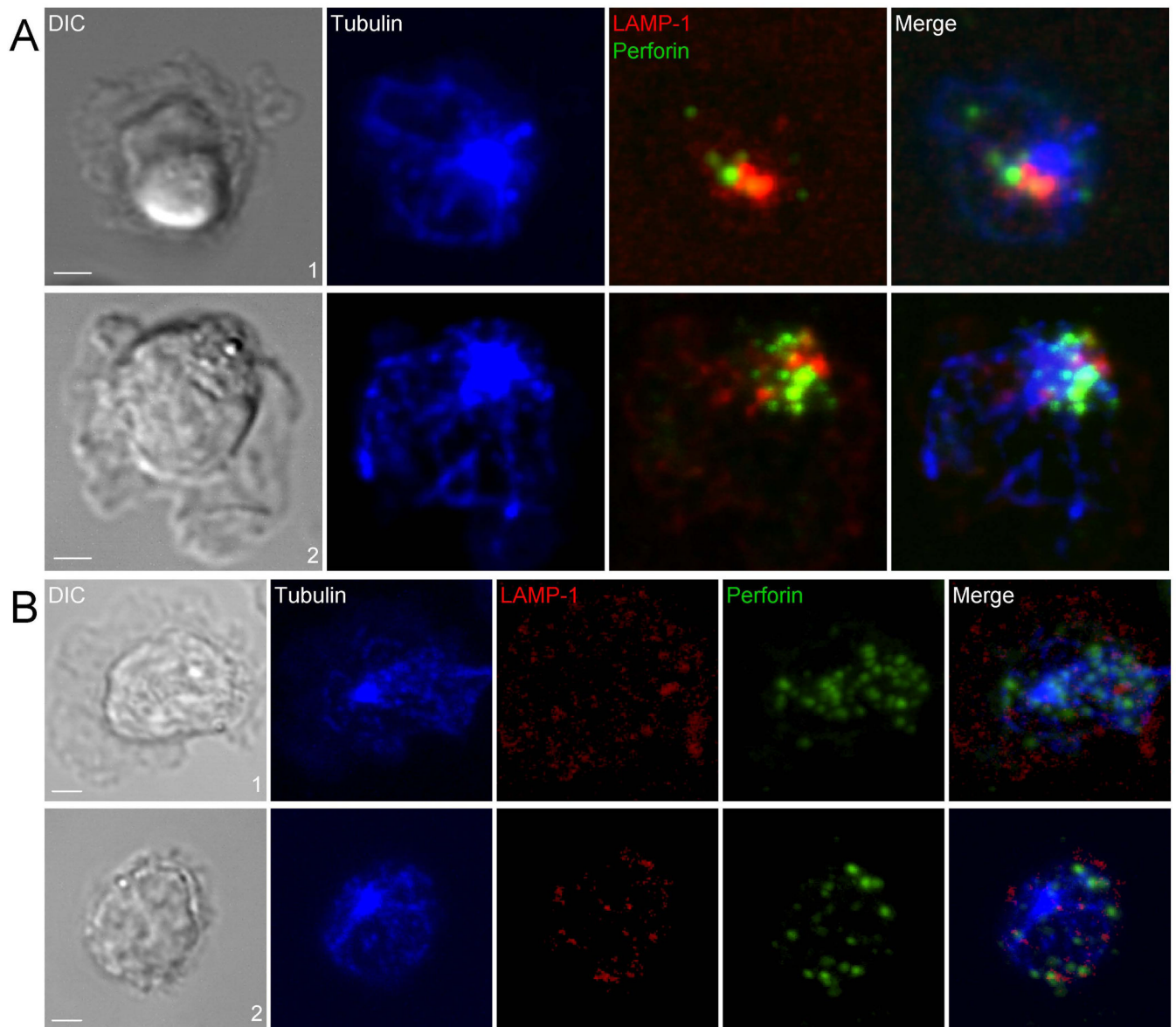


Figure 7. Polarized Perforin-Containing Lytic Granules Contact Internalized LAMP-1 in the Presence of ICAM-1

(A) NK cells imaged on bilayers containing Fc and ICAM-1 ~60 min (#1) and ~120 min (#2) after injection over the bilayer. Perforin (Green), internalized LAMP-1 (Red), and Tubulin (Blue) were acquired by 3D confocal microscopy. Scale bars are 5.0 μm . The images are representative of at least 30 cells in two independent experiments. (B) NK cells imaged on bilayers carrying Fc ~120 min after injection over bilayer. Differential interference contrast (DIC) images are shown on the *Left*. Merged overlays of fluorescent are on the *Right*. LAMP-1 (Red) detected by inclusion of 0.016 μM Alexa Fluor 647-labeled CD107a Fab during NK cell incubation on with lipid bilayer containing Fc, MTOC (Blue) and perforin (Red) are shown in *Center*. Scale bars are 2.0 μm . The images are representative of 50 cells in three independent experiments.